Intrinsic Distortion of a Fully Differential BD-Modulated Class-D Amplifier with Analog Feedback

Stephen M. Cox, Jun Yu, Wang Ling Goh, and Meng Tong Tan

***Abstract*—This paper presents a mathematical analysis of a fully differential BD-modulated Class-D amplifier with analog feedback, i.e., one having a bridge-tied-load output configuration with negative feedback and ternary PWM signal. Notwithstanding the highly nonlinear nature of the amplifier's operation, an extremely accurate closed-form expression for the audible output signal is derived and verified based on computer simulations. This expression demonstrates that there exist larger high-order intrinsic distortions (e.g., 5th-order harmonic distortion and intermodulation distortion) for BD-modulation, compared to that for AD-modulation (binary PWM signal). Furthermore, the 3rd-order harmonic distortion has a roughly parabolic response as a function of the magnitude of the input signal and reaches its peak when the modulation index of the input signal is around 0.7. Overall, the BD-modulated Class-D amplifier has a larger intrinsic distortion for small input signal but a smaller intrinsic distortion for large input signal, compared to AD-modulated designs.**

***Index Terms*—BD modulation, bridge-tied-load (BTL), filterless Class-D amplifier, differential-ended, intermodulation distortion (IMD), time-domain analysis, total harmonic distortion (THD).**

EDICS Category: ACS350, ACS130, ACS100, NOLIN150

I. Introduction

CLASS-D amplifiers have rapidly supplanted linear amplifiers in recent years, both for low-power and high-power devices [1]. Their adoption has been motivated by their high efficiency. Although a variety of modulation topologies have been developed for the analog-feedback Class-D amplifier, the traditional pulse width modulation (PWM) scheme is still widely used due to its fixed and moderate switching frequency.

As proposed in [2], a pulse width modulated Class-D amplifier can be further categorized into two types: AD modulation (or Class-AD) and BD modulation (or Class-BD). The PWM signal for AD modulation takes only two values, e.g., plus/minus supply voltage, and hence it is also referred to as binary modulation. By contrast, the PWM signal for BD modulation takes three values, e.g., plus/minus supply voltage and ground, and so is named ternary modulation. AD modulation is dominant for single-ended output configurations. BD modulation is usually realized with a differential-ended output stage, yielding a so-called bridge-tied-load (BTL) configuration. Furthermore, as the carrier frequency components of the two half bridges are in phase, BD modulation has much lower differential-mode high-frequency current ripple loss, compared to AD modulation. This is essential for a "filterless" Class-D amplifier to achieve high power efficiency when the LC filter is minimized or even completely removed.

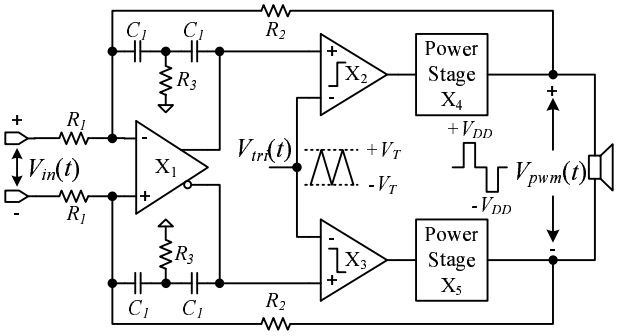

Fig. 1. Circuit schematic of a fully differential BD-modulated Class-D amplifier.

Fig. 1 shows a popular circuit structure for a 2nd-order Class-D amplifier applying BD modulation and with analog feedback. The output stage is differential-ended and the carriers of both bridge halves are in-phase, whereas the modulating signals are generated from a fully-differential 2nd-order loop filter and hence have opposite phase. The optional output LC filter is omitted, as it does not affect the analysis presented in this work. Fully differential loop filters have been widely employed in the recent works [3]–[6], although their implementation is not limited to the structure shown in Fig. 1. For instance, the 2nd-order loop filter may in fact comprise two 1st-order integrators, as demonstrated in [5], and the input resistors can be replaced by a differential operational transconductance amplifier (OTA), as in [6].

Furthermore, there are some BD-modulated Class-D amplifiers reported in the literature that are built using pseudo-differential loop filters, in which two single-ended loop filters are employed, one for each bridge half. Consequently, the circuit is exactly a combination of two single-ended AD-modulated Class-D amplifiers. The audible frequency compo-

Stephen M. Cox is with the School of Mathematical Sciences, University of Nottingham, Nottingham NG7 2RD, UK (email: stephen.cox@nottingham.ac.uk).

Jun Yu and Wang Ling Goh are with the School of Electrical and Electronic Engineering, Nanyang Technological University, Singapore 639798 (e-mail: yu0002un@ntu.edu.sg ; ewlgoh@ntu.edu.sg).

Meng Tong Tan is with the Agency for Science, Technology and Research (A*STAR), Institute of Microelectronics (IME), Singapore 117685 (email: mengtong.tan@ieee.org).

nents of such pseudo-differential BD modulation are therefore the same as those for AD modulation, except that the output swing is doubled. Thus, in the present work, we are interested only in BD-modulated Class-D amplifiers with fully differential loop filter.

The performance of PWM Class-D amplifiers has been significantly improved in the last decade. This improvement has mainly been driven by the advancement of power MOSFET fabrication technology, as well as optimized circuit implementation. The total harmonic distortion (THD) reported in the recent works [1], [4], [5] has reached around 0.01%, at which level the intrinsic distortion due to the feedback loop structure becomes a limiting factor for linearity whenever the designer wishes to use a low switching frequency to ensure a high power efficiency. Some attempts at reducing the intrinsic harmonic distortion have been reported [3], [7]–[9]. In [8] (see also [10]), a sample-and-hold block added after the loop filter was proposed, to reduce the intrinsic harmonic distortion. This idea was recently implemented in a BD-modulated Class-D amplifier [3] and an impressive THD of 0.00122% at 1 kHz and 50% maximum output power was achieved.

While BD modulation has been widely accepted by the industry, a comprehensive mathematical analysis of this topology is not available in the literature; indeed it is highly nontrivial. As we investigate in this paper, the intrinsic distortion of a BD-modulated closed-loop Class-D amplifier is quite different from that of an AD-modulated design. To be more precise, BD modulation causes higher intrinsic distortion for small input signals, but has less intrinsic distortion for large input signals. Interestingly, its 3rd-order harmonic has a roughly parabolic response as a function of the magnitude of the input signal. In addition, BD modulation suffers larger high-order harmonic distortion, compared to AD modulation, e.g., the 5th-order harmonic may be even larger than the 3rd-order harmonic. According to audio engineers, human beings are quite sensitive to high-order harmonic distortion, compared to low-order harmonic distortion. This may be a potential drawback of BD modulation.

This paper is organized as follows. In Section II, we briefly review the prior analysis of Class-D amplifiers, especially focusing on the intrinsic distortion for a closed-loop design. In Section III, the major steps in analyzing the BD-modulation design are summarized, and an explicit amplifier output expression is derived. In Section IV, the closed-form expressions for the intrinsic distortion, in the form of total harmonic distortion (THD) and intermodulation distortion (IMD) are derived and analyzed. In Section V, we compare our analytical results with simulations of the amplifier, and demonstrate the excellent agreement. Finally, we give our conclusions in Section VI.

II. Literature Review

The analysis of Class-D amplifiers can be traced back to the 1950s [11]. There, a double Fourier series was applied to derive an expression for the output signal of an open-loop Class-D amplifier with either natural or uniform sampling. This series demonstrated that an ideal open-loop naturally sampled PWM Class-D amplifier does not introduce any harmonic distortion in the audio band. This conclusion is extended to an arbitrary band-limited input signal in [12]. However, due to component variation, non-ideal power stage and distorted carrier signal [13], the THD for practical open-loop Class-D amplifiers is typically 0.1%. Therefore, negative feedback is widely applied in commercial products to improve the linearity of open-loop Class-D amplifiers.

However, it is also well known that a closed-loop pulse width modulated Class-D amplifier has intrinsic distortion due to the injection of high-frequency carrier ripples at the output of the loop filter. The ripple signal contains high frequency intermodulation products between the input and carrier signals. The input-dependent ripple signal causes timing errors at the rising and falling edges of the PWM signal and hence generates distortion in the demodulated output signal. Put more abstractly, the intrinsic distortion is caused by the circuit structure itself and is not related to practicalities of circuit construction.

Various analyses of this intrinsic distortion phenomenon of a closed-loop Class-D amplifier have been reported in recent years [7], [10], [14], [15], focusing only on AD modulation (binary PWM signal). The analysis in [7] provides an insight into the source of the intrinsic distortions, and the derivation process closely reflects the working mechanism of the system. It gives an expression for the output which is valid for a general input signal (followed by a more detailed treatment of the case of sinusoidal input, capturing the third-harmonic distortion terms), at modest algebraic cost. (An extension of the analysis in [7] to self-oscillating designs was reported in [16].) In our previous work [10], [14], we introduced an alternative time-domain analysis technique that is able to precisely predict the intrinsic harmonic distortion of an AD-modulated Class-D amplifier with either 1st-order or 2nd-order loop filter. The essential mathematical tool for this calculation is a perturbation method based on the small ratio between typical audio frequencies and the amplifier switching frequency. The advantages of this technique are: 1) that the output signal is obtained analytically for any band-limited input signal, in a compact form, 2) that the derivation procedure is systematic and hence the analytical expression can in principle be obtained to any desired precision, and 3) that the order of magnitude of the errors that arise from computing only the first few terms in the perturbation expansion can be estimated.

In this paper, we will extend this technique to the fully differential BD-modulated closed-loop Class-D amplifier. Due to the ternary stage of the output signal, the analytical work is even more complex than previous treatments, involving much heavy algebra, which is relegated to a computer algebra package. The value of this analysis is that it yields a closed-form expression for the audio-frequency components of the amplifier output, which allows us to investigate the unique properties of the BD modulation. To our knowledge, this is the first analytical work on the output spectrum of BD modulation, although it was first introduced in the 1970s and has been widely used for nearly one decade for audio amplifiers.

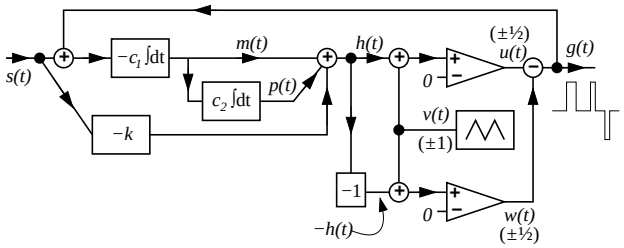

Fig. 2. Fully differential BD-modulated Class-D amplifier with negative feedback and BTL output configuration. See text for details.

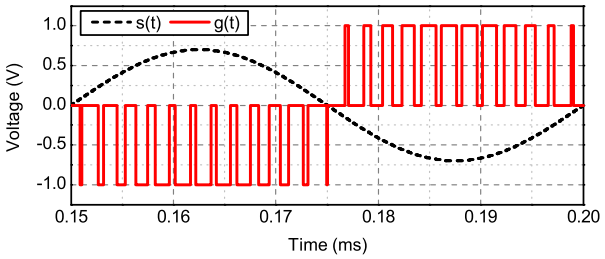

Fig. 3. Waveforms for typical operation of the amplifier. Note that the amplifier output $g(t)$ alternates between 0 and -1 when $s(t) > 0$ and between 1 and 0 when $s(t) < 0$.

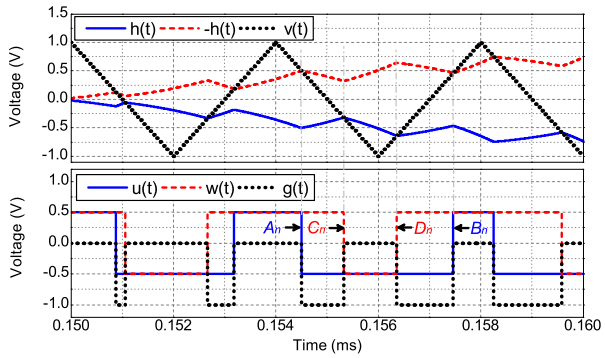

Fig. 4. Waveforms for typical operation of the amplifier.

III. Mathematical Analysis of BD Modulation

Fig. 2 shows the mathematical model that we have derived for the BD-modulated Class-D amplifier illustrated in Fig. 1. As in our previous work [14], we have added a constant gain block (i.e., equal to $-k$) into the mathematical model to represent a feedforward path from the input signal to the loop filter output signal. Although this feedforward path is not shown in Fig. 1, it can be easily realized by creating an extra input port at each comparator. In addition, this model is suitable for both first-order (i.e., $c_2 = 0$) and second-order (i.e., $c_2 > 0$) loop filter designs. In this work, we focus on the second-order loop filter design as it provides a higher linearized loop gain and hence can significantly suppress the distortion caused by the power stage. However, the output expression for first-order design is also provided at the end of this section, for completeness. Expressions for the model parameters c_1 and c_2, and the input signal, $s(t)$, (all indicated in Fig. 2) are given in Table I, where the passive components and the signals refer to the circuit schematic shown in Fig. 1.

TABLE I
Mathematical Model Parameters

Model Parameter	Expression
c_1	$(V_{DD}/V_T)(1/(R_2C_1))$
c_2	$1/(2R_3C_1)$
$s(t)$	$(R_2/R_1)(1/V_{DD})V_{in}(t)$

A. Formulation of the Model

The input to the device is an audio signal, $s(t)$, of relatively low frequency. Throughout this paper, voltages are scaled so that $s(t)$ lies in the range $-1 < s(t) < 1$. The amplifier output is a high-frequency square-wave PWM signal, $g(t)$, taking the values -1, 0 and 1. As illustrated in Fig. 2, the signals $s(t)$ and $g(t)$ are summed and this sum is integrated twice, in succession, yielding signals $m(t)$ and $p(t)$, which satisfy

$$\frac{\mathrm{d}m(t)}{\mathrm{d}t} = -c_1(s(t) + g(t)), \qquad \frac{\mathrm{d}p(t)}{\mathrm{d}t} = c_2 m(t), \quad (1)$$

where c_1 and c_2 are positive constants.

Next, $m(t)$ and $p(t)$ are summed with a multiple of the original audio signal, $-ks(t)$, and with a high-frequency triangular carrier wave $v(t)$ of period T; this sum is fed to the noninverting input of a comparator, whose inverting input is at zero volts. The carrier wave is given by

$$v(t) = \begin{cases} 1 - 4t/T & \text{for } 0 \le t < \frac{1}{2}T, \\ -3 + 4t/T & \text{for } \frac{1}{2}T \le t < T, \end{cases} \quad (2)$$

together with the periodicity condition $v(t+T) = v(t)$. The comparator output voltage is given by

$$u(t) = \begin{cases} +1/2 & \text{if } m(t) + p(t) - ks(t) + v(t) > 0, \\ -1/2 & \text{if } m(t) + p(t) - ks(t) + v(t) < 0. \end{cases} \quad (3)$$

Also, the sum $h(t) = m(t) + p(t) - ks(t)$ is inverted, added to the carrier wave and fed to a second comparator, whose output is given by

$$w(t) = \begin{cases} +1/2 & \text{if } -(m(t) + p(t) - ks(t)) + v(t) > 0, \\ -1/2 & \text{if } -(m(t) + p(t) - ks(t)) + v(t) < 0. \end{cases} \quad (4)$$

The output of the amplifier is given by $g(t) = u(t) - w(t)$:

$$g(t) = \begin{cases} +1 & \text{if } |v(t)| < m(t) + p(t) - ks(t), \\ 0 & \text{if } -|v(t)| < m(t) + p(t) - ks(t) < |v(t)|, \\ -1 & \text{if } m(t) + p(t) - ks(t) < -|v(t)|. \end{cases} \quad (5)$$

Finally, this output is fed back to the input of the amplifier, providing negative feedback.

Fig. 3 shows the typical waveform of the output differential PWM signal, $g(t)$, corresponding to a sinusoidal input signal, $s(t)$. Note that $g(t)$ switches between -1 and 0 when $s(t) > 0$, and between 0 and 1 when $s(t) < 0$. A zoomed-in view of the internal control signals ($\pm h(t)$ and $v(t)$) and the two comparator output signals ($u(t)$ and $w(t)$) is illustrated in Fig. 4

for the time interval from 0.15 ms to 0.16 ms of Fig. 3. These figures show that $u(t)$ and $w(t)$ each switch twice during one carrier-wave period, with $g(t)$ switching correspondingly four times. We denote the times at which the comparator outputs switch between the values $\pm\frac{1}{2}$ by A_n, B_n, C_n and D_n, for integers n, where $nT < A_n, B_n, C_n, D_n < (n+1)T$. More specifically,

$$u(t) = \begin{cases} +1/2 & \text{for } B_{n-1} < t < A_n, \\ -1/2 & \text{for } A_n < t < B_n \end{cases} \tag{6}$$

and

$$w(t) = \begin{cases} +1/2 & \text{for } D_{n-1} < t < C_n, \\ -1/2 & \text{for } C_n < t < D_n. \end{cases} \tag{7}$$

In writing (6) and (7), we assume normal operation, i.e., that each comparator switches twice during each carrier-wave period, as observed in simulations. (For sufficiently large signal amplitudes, occasional pulses may be skipped in some other Class-D amplifier designs, leading to a degradation in performance; however, we have not observed pulse-skipping in the present design. A discussion of the "large-signal" stability of an AD-modulated Class-D amplifier can be found in [14].)

It proves useful to introduce the fractional switching times α_n, β_n, γ_n and δ_n, given by $A_n = (n+\alpha_n)T$, $B_n = (n+\beta_n)T$, $C_n = (n+\gamma_n)T$, $D_n = (n+\delta_n)T$, where

$$0 < \alpha_n < \tfrac{1}{2} < \beta_n < 1, \qquad 0 < \gamma_n < \tfrac{1}{2} < \delta_n < 1. \tag{8}$$

Finally, in view of the need, from (1), to integrate the input signal twice, we introduce $f(t)$ such that $s(t) = f''(t)$.

B. Structure of the Calculation

The present BD modulation design is more complicated to analyze than previously considered AD modulation designs [14]. In part this is because the output $g(t)$ switches four times per carrier-wave period. However, the more significant complication, for the mathematical model, is that the relative *order* of the switchings of $u(t)$ and $w(t)$ differs, depending on the sign of $s(t)$. Below, we present a detailed analysis for the case $s(t) > 0$, for which the order of switchings is

$$\cdots < A_n < C_n < D_n < B_n < A_{n+1} < \cdots . \tag{9}$$

For the case $s(t) < 0$, the order of switching is $\cdots < C_n < A_n < B_n < D_n < C_{n+1} < \cdots$ and consequent modifications to the account below are readily worked out.

The details of the calculation are highly algebraically involved, and it is useful to highlight the structure of the calculation, as follows. First, we integrate (1) from $t = A_n$ to $t = A_{n+1}$, across each of the subintervals indicated in (9), noting that $g(t)$ is constant in each subinterval; specifically,

$$g(t) = \begin{cases} -1 & \text{for } A_n < t < C_n \text{ or } D_n < t < B_n, \\ 0 & \text{otherwise.} \end{cases} \tag{10}$$

Thus we obtain

$$\begin{aligned}
m(C_n) &= m(A_n) - c_1(f'(C_n) - f'(A_n)) + c_1(C_n - A_n), \\
p(C_n) &= p(A_n) + c_2 m(A_n)(C_n - A_n) - \mathcal{F}(A_n, C_n) \\
&\quad + \tfrac{1}{2}c_1c_2(C_n - A_n)^2, \\
m(D_n) &= m(C_n) - c_1(f'(D_n) - f'(C_n)), \\
p(D_n) &= p(C_n) + c_2 m(C_n)(D_n - C_n) - \mathcal{F}(C_n, D_n), \\
m(B_n) &= m(D_n) - c_1(f'(B_n) - f'(D_n)) + c_1(B_n - D_n), \\
p(B_n) &= p(D_n) + c_2 m(D_n)(B_n - D_n) - \mathcal{F}(D_n, B_n) \\
&\quad + \tfrac{1}{2}c_1c_2(B_n - D_n)^2, \\
m(A_{n+1}) &= m(B_n) - c_1(f'(A_{n+1}) - f'(B_n)), \\
p(A_{n+1}) &= p(B_n) + c_2 m(B_n)(A_{n+1} - B_n) - \mathcal{F}(B_n, A_{n+1}),
\end{aligned}$$

where $\mathcal{F}(t_1, t_2) = c_1c_2(f(t_2) - f(t_1) - f'(t_1)(t_2 - t_1))$.

It is then straightforward, if algebraically messy, to eliminate the intermediate values of m and p and hence obtain difference equations, of the form

$$m_{n+1} = \mathcal{M}(n, m_n, p_n, \alpha_n, \beta_n, \gamma_n, \delta_n, \alpha_{n+1}), \tag{11}$$

$$p_{n+1} = \mathcal{P}(n, m_n, p_n, \alpha_n, \beta_n, \gamma_n, \delta_n, \alpha_{n+1}), \tag{12}$$

where m_n denotes $m(A_n)$ and p_n denotes $p(A_n)$.

The switching times are determined, according to (3), (4), (6) and (7), from

$$m(A_n) + p(A_n) - ks(A_n) + 1 - 4\alpha_n = 0, \tag{13}$$

$$m(B_n) + p(B_n) - ks(B_n) - 3 + 4\beta_n = 0, \tag{14}$$

$$-m(C_n) - p(C_n) + ks(C_n) + 1 - 4\gamma_n = 0, \tag{15}$$

$$-m(D_n) - p(D_n) + ks(D_n) - 3 + 4\delta_n = 0. \tag{16}$$

The six equations (11)–(16) constitute a set of governing difference equations for the amplifier. They can be used as the basis for accurate numerical simulations of the amplifier (cf. [17], [18]), but, more importantly, they can be used to predict a closed-form expression for the audio output of the amplifier in response to a general audio input, as we now demonstrate.

C. Solving the Model

The key to a mathematical analysis of the difference-equation model (11)–(16) is the observation that the carrier-wave frequency greatly exceeds a typical audio frequency (typically 500kHz and 20Hz–20kHz, respectively). Thus each voltage in the amplifier may be considered to oscillate at the carrier-wave frequency, with a slow modulation. To make this idea more precise, we introduce the small parameter

$$\epsilon \equiv \omega T \ll 1, \tag{17}$$

where ω is a typical audio (angular) frequency, and the (dimensionless) slow time scale

$$\tau = \omega t = \epsilon t/T. \tag{18}$$

To acknowledge the relatively slow variation of the audio signal, we also write $s(t) = S(\tau) = \mathrm{d}^2F(\tau)/\mathrm{d}\tau^2$, where $F(\tau) = \epsilon^2 f(t)/T^2$. The presence of a small parameter in the problem allows us to use perturbation methods to solve the mathematical model.

We next introduce six functions that are to be determined from (11)–(16): these represent the four switching times in a given switching period, together with the values of the integrator outputs sampled at times $t = A_n$. Thus we introduce the functions $\alpha(\tau)$, $\beta(\tau)$, $\gamma(\tau)$, $\delta(\tau)$, $m(\tau)$ and $p(\tau)$, such that

$$(\alpha(\epsilon n), \beta(\epsilon n), \gamma(\epsilon n), \delta(\epsilon n), m(\epsilon n), p(\epsilon n)) = (\alpha_n, \beta_n, \gamma_n, \delta_n, m_n, p_n).$$

Furthermore, we expand each function in powers of ϵ, so that

$$\alpha(\tau) = \sum_{n=0}^{\infty} \epsilon^n \alpha^{(n)}(\tau), \quad \beta(\tau) = \sum_{n=0}^{\infty} \epsilon^n \beta^{(n)}(\tau), \quad \text{etc.}, \tag{19}$$

and solve the problems that arise from substituting these functions into (11)–(16) at successive powers of ϵ.

At leading order, after much algebra, we find the fractional switching times to be given by

$$\begin{aligned}
\alpha^{(0)}(\tau) &= \tfrac{1}{16}(1 - S(\tau))(4 - c_1 T S(\tau)),\\
\beta^{(0)}(\tau) &= \alpha^{(0)}(\tau) + \tfrac{1}{2}(1 + S(\tau)),\\
\gamma^{(0)}(\tau) &= \alpha^{(0)}(\tau) + \tfrac{1}{2} S(\tau),\\
\delta^{(0)}(\tau) &= \alpha^{(0)}(\tau) + \tfrac{1}{2},
\end{aligned}$$

while the sampled values of the integrator outputs are

$$m^{(0)}(\tau) = -\tfrac{1}{4} c_1 T S(\tau)(1 - S(\tau)), \quad p^{(0)}(\tau) = -(1-k) S(\tau). \tag{20}$$

From (10), the average of $g(t)$ over a carrier-wave period is

$$-\beta^{(0)}(\tau) + \delta^{(0)}(\tau) - \gamma^{(0)}(\tau) + \alpha^{(0)}(\tau) = -S(\tau) = -s(t). \tag{21}$$

Thus, to a good approximation, the audio-frequency component of the amplifier output is the inverted audio input signal.

In order to make useful predictions about the amplifier distortion, it is necessary to proceed in succession to terms of orders ϵ, ϵ^2 and ϵ^3. The volume of algebra necessary to analyze these problems grows rapidly; since it is really only the final answer that is of practical significance, we record none of the detailed intermediate results here.

Once the first few terms in the expansions for the functions α, β, γ and δ have been found, the final step in the calculation is to extract from the switching times the audio components that are present in $g(t)$. Extending the approach used previously in [14], we find that the audio-frequency components of the output, which we denote by $g_a(t)$, are given by (cf. [12], [19])

$$g_a(t) = \sum_{n=1}^{\infty} \frac{(-\epsilon)^{n-1}}{n!} \frac{\mathrm{d}^{n-1}}{\mathrm{d}\tau^{n-1}} (\alpha^n(\tau) + \delta^n(\tau) - \beta^n(\tau) - \gamma^n(\tau)). \tag{22}$$

Calculating terms up to order ϵ^3, then rewriting the answer in terms of $s(t)$, the output expression is finally derived as

$$\begin{aligned}
g_a(t) = -s(t) &+ T^2 \frac{\mathrm{d}^2}{\mathrm{d}t^2} \left\{ \left[-\frac{1}{48} + \frac{1-k}{c_1 c_2 T^2} \right] s(t) - \tfrac{1}{24} s^3(t) \right\}\\
&+ \tfrac{1}{16} T^2 \frac{\mathrm{d}^2 (s^2(t))}{\mathrm{d}t^2} \operatorname{sgn}(s(t)),
\end{aligned} \tag{23}$$

where $\operatorname{sgn}(s)$ equals 1 for $s > 0$, and -1 for $s < 0$.

Equation (23) is of particular importance because it accurately predicts the audible output components for BD modulation and is suitable for an arbitrary band-limited input signal. If we compare (23) with the output signal expression in [14], the similarities and differences between the audible output signals for AD and BD modulation may be interpreted as follows.

Similarities—The terms in the first line of (23) are exactly as for the AD-modulated second-order design analyzed in [14]. The term $(s(t))''$ contributes only to the distortion of the fundamental frequency components, causing the magnitude of the fundamental frequency components to slightly increase. Also, the feedforward path (i.e., $-k$) can be used to compensate the distortion of the fundamental output components.

Differences—The quadratic term in the second line of (23), i.e., $\frac{1}{16} T^2 (s^2(t))'' \operatorname{sgn}(s(t))$, is new, and unique to BD modulation. This term reflects the change in the relative switching order of the two bridge halves for positive and negative values of $s(t)$ and significantly affects the intrinsic distortion components that are appreciably present in the output. Note that this term is a product of an even function of the input signal, $(s^2(t))''$, and an odd function, $\operatorname{sgn}(s(t))$. As a result, it will generate only odd-order harmonics, with magnitudes proportional to the square of the input signal magnitude.

It may also be worthwhile to highlight that the terms $(s^3(t))''$ and $(s^2(t))'' \operatorname{sgn}(s(t))$ in (23) are the source of harmonics and intermodulation products in the demodulated output signal. As these two terms are independent of the loop filter parameters (i.e., c_1 and c_2), we conclude that, up to the order of the analysis (i.e., ϵ^3), the THD and IMD of the BD-modulated Class-D amplifier are independent of the design of the loop filter. We recall that the same property also holds for AD modulation [14].

The audible output expression for first-order loop filter design (i.e. $c_2 = 0$) has been derived in the same way, and is

$$\begin{aligned}
g_a(t) = -s(t) &+ \frac{1-k}{c_1} \frac{\mathrm{d}s}{\mathrm{d}t} - \tfrac{1}{32} T^2 \frac{\mathrm{d}^2 (s^2(t))}{\mathrm{d}t^2} \operatorname{sgn}(s(t))\\
&+ T^2 \frac{\mathrm{d}^2}{\mathrm{d}t^2} \left\{ \left[\frac{1}{48} - \frac{1-k}{c_1^2 T^2} \right] s(t) + \tfrac{1}{48} s^3(t) \right\}.
\end{aligned} \tag{24}$$

As the coefficients for the nonlinear terms in (24) are exactly half of those in (23), the intrinsic distortion components for the first-order design have the same trend as for the second-order design, except that the magnitude is reduced by half. For the sake of brevity, the analysis in the following sections of this work is based only on the second-order design. It is worth noting that the coefficients of the cubic terms in (23) and (24) agree with the corresponding results in [7]; furthermore, the finding that this component of the intrinsic distortion is reduced by half for the purely first-order design is also in accordance with [7].

IV. Intrinsic Distortion of a BD-modulated Class-D Amplifier

In this section, we will examine the intrinsic distortion of a BD-modulated closed-loop Class-D amplifier for both single-tone and two-tone input signals, in the form of THD and IMD, respectively. Due to the $\operatorname{sgn}(s(t))$ function, this derivation

procedure is rather mathematically involved. To simplify the presentation, only the final expressions are presented here, with some important details attached in the Appendix.

A. Total Harmonic Distortion

For a single-tone audio input signal, a nonlinear amplifier gives rise to an audio output that can be expressed as

$$g_a(t) = \sum_{n=-\infty}^{\infty} g_n \mathrm{e}^{nj\omega t}. \tag{25}$$

Then the total harmonic distortion is defined as

$$\mathrm{THD}(\%) = \sqrt{|g_2|^2 + |g_3|^2 + \cdots}/|g_1| \times 100. \tag{26}$$

By substituting the audio signal, $s(t) = s_0 \sin \omega t$, into (23), $g_a(t)$ may be derived as

$$-s_0\left\{1 + (\omega T)^2\left[\left(-\frac{1}{48} + \frac{1-k}{c_1 c_2 T^2}\right) - \tfrac{1}{32}s_0^2\right]\right\}\sin \omega t$$
$$- \tfrac{3}{32}(\omega T)^2 s_0^3 \sin 3\omega t + (\omega T)^2 s_0^2 \sum_{\text{odd } n} \frac{n \sin n\omega t}{2\pi(n^2-4)}. \tag{27}$$

Note that, in contrast to AD modulation, there exist significant high-order odd harmonics in the output of a BD-modulated Class-D amplifier, which are represented by the summation term in (27). In addition, we note that the third-harmonic distortion term has coefficient $3(\omega T)^2 s_0^2(\frac{1}{10\pi} - \frac{1}{32}s_0)$, which has a maximum at $s_0 = \frac{32}{15\pi} \approx 0.679$. Furthermore, the third-harmonic distortion of the BD modulation is *greater* than that of the single-ended design (AD modulation) unless the audio signal amplitude is sufficiently large, specifically unless $s_0 > \frac{8}{5\pi} \approx 0.509$.

If we include *all* generated harmonics from (27), we find

$$\mathrm{THD} \sim (\omega T)^2 s_0 \left\{\left(\tfrac{3}{10\pi} - \tfrac{3}{32}s_0\right)^2 + \sum_{\text{odd } n \geq 5} \frac{n^2}{4\pi^2(n^2-4)^2}\right\}^{1/2}$$
$$\sim (\omega T)^2 s_0 \left\{\left(\tfrac{3}{10\pi} - \tfrac{3}{32}s_0\right)^2 + \tfrac{1}{64}\left(1 - \tfrac{1696}{225\pi^2}\right)\right\}^{1/2}. \tag{28}$$

Consideration of this expression shows that the THD of a BD-modulated Class-D amplifier increases with increasing signal amplitude s_0. As with the third-harmonic distortion, this amplifier has *greater* THD than its AD-modulated counterpart for small signal amplitudes; the present design has lower THD only when $s_0 > 5(9\pi^2 - 16)/(162\pi) \approx 0.715$. Of course, it should be borne in mind that the higher harmonics generated by the amplifier will be beyond the range of human hearing, so the infinite sum implicit in (28) should be (generally severely) truncated. If such a truncation is made, it still remains the case that the THD increases with increasing s_0 (unless we keep only the third harmonic term, in which case the THD has a maximum at $s_0 = \frac{32}{15\pi}$, as above).

Fig. 5 illustrates the output spectrum of a BD-modulated 2nd-order Class-D amplifier based on MATLAB simulation. The input signal is set at 1 kHz with modulation index equal to 0.7. The carrier frequency is set to 250 kHz, which will be the default value in the rest of the paper (in the absence of specification to the contrary). This figure clearly shows

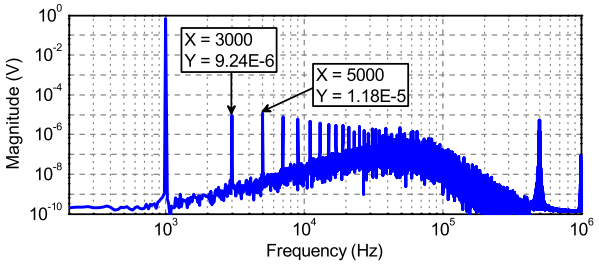

Fig. 5. Frequency spectrum of the demodulated output signal of the Class D amplifier with BD modulation. The input signal is set to have frequency $F_{\text{in}} = 1$ kHz and modulation index $M_{\text{in}} = 0.7$. Carrier frequency is set to 250 kHz.

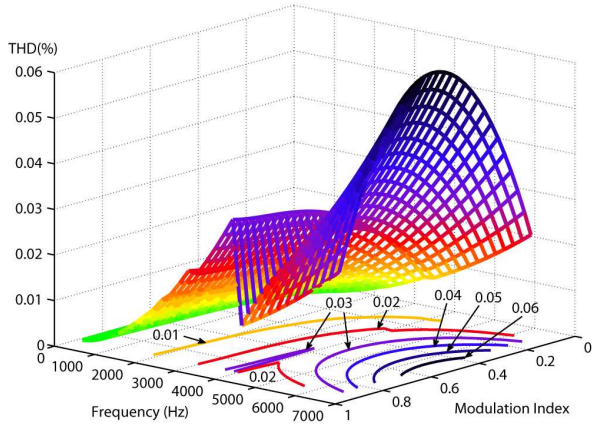

Fig. 6. 3D plot of the THD of a BD-modulated Class-D amplifier as a function of both the modulation index and frequency of the input signal.

that there exist significant high-order harmonic components in the output spectrum. It is particularly noteworthy that the 5th harmonic is in this case larger than 3rd harmonic. This indicates that the BD-modulated Class-D amplifier has an output spectrum that is quite different from that for AD modulation.

Using (27), we are able to predict the THD performance of a BD-modulated Class-D amplifier, with relatively little computational effort, and without the need for numerous time-consuming simulations. Fig. 6 shows a three-dimensional plot of the THD with respect to both the modulation index and the frequency of the input signal. The data are calculated based on our analytical expression, including all significant harmonics within the 20 kHz audio band. The corresponding contour lines with 0.01% THD incremental step are plotted on the base of the 3D diagram.

B. Intermodulation Distortion

Intermodulation distortion (IMD) arises when the amplifier input comprises multiple signals with different frequencies. The output then contains contributions at sums and differences of the various frequencies. IMD can significantly detract from the listening experience.

We thus consider the IMD for an input signal

$$s(t) = s_1 \sin \omega_1 t + s_2 \sin \omega_2 t \qquad (s_1, s_2 > 0). \tag{29}$$

For such a signal, the output may be written as

$$g_a(t) = \sum_{m=-\infty}^{\infty} \sum_{n=-\infty}^{\infty} g_{m,n} \mathrm{e}^{\mathrm{j}(m\omega_1 + n\omega_2)t}, \tag{30}$$

and the "order" of a given intermodulation product (IMP) is defined as $|m| + |n|$. Then the IMD of order K is

$$\mathrm{IMD}_K(\%) = \frac{1}{|g_{0,1}|} \sqrt{\sum |g_{m,n}|^2} \times 100, \tag{31}$$

where the sum is taken over all IMP with order less than or equal to K.

The contribution to the IMD from the terms in the first line of (23) may be expressed as

$$\sum G_{m,n} \sin(m\omega_1 + n\omega_2)t, \tag{32}$$

where the nonzero coefficients are

$$\begin{aligned}
G_{1,0} &= -(1 + \mu\omega_1^2 T^2)s_1 + \tfrac{1}{32} s_1^3 \omega_1^2 T^2 + \tfrac{1}{16} s_1 s_2^2 \omega_1^2 T^2, \\
G_{0,1} &= -(1 + \mu\omega_2^2 T^2)s_2 + \tfrac{1}{32} s_2^3 \omega_2^2 T^2 + \tfrac{1}{16} s_1^2 s_2 \omega_2^2 T^2, \\
G_{3,0} &= -\tfrac{3}{32} s_1^3 \omega_1^2 T^2, \qquad G_{0,3} = -\tfrac{3}{32} s_2^3 \omega_2^2 T^2, \\
G_{2,\pm 1} &= -\tfrac{1}{32} s_1^2 s_2 (2\omega_1 \pm \omega_2)^2 T^2, \\
G_{1,\pm 2} &= -\tfrac{1}{32} s_1 s_2^2 (\omega_1 \pm 2\omega_2)^2 T^2,
\end{aligned}$$

and where $\mu = -\frac{1}{48} + (1-k)/(c_1 c_2 T^2)$. Recall that the intermodulation products generated by the first line of (23) are consistent with those of an AD-modulated Class-D amplifier [20].

The corresponding calculation for the term $\frac{1}{16} T^2 (s^2(t))'' \operatorname{sgn}(s(t))$ in the second line of (23) is more complicated; for this we use the method of Bennett [21], [22]. The detailed derivation is given in the Appendix, with the final expression for $g_a(t)$ being

$$\begin{aligned}
&-\tfrac{1}{16} T^2 \sigma (\omega_1^2 s_1 \sin\omega_1 t + \omega_2^2 s_2 \sin\omega_2 t) \\
&+\tfrac{1}{16} T^2 \sigma^2 \sum_{p=1}^{\infty} \sum_{\substack{q=-\infty \\ p+q \text{ odd}}}^{\infty} (p\omega_1 + q\omega_2)^2 \mathcal{H}_{pq} \sin(p\omega_1 + q\omega_2)t \\
&+\tfrac{1}{16} T^2 \sigma^2 \sum_{\substack{q=1 \\ q \text{ odd}}}^{\infty} q^2 \omega_2^2 \mathcal{H}_{0q} \sin q\omega_2 t,
\end{aligned} \tag{33}$$

where

$$\mathcal{H}_{pq} = \sum_{\substack{n=1 \\ n \text{ odd}}}^{\infty} \frac{16}{n^3 \pi^3} \mathrm{J}_p(n\pi s_1/\sigma) \mathrm{J}_q(n\pi s_2/\sigma), \tag{34}$$

and $\sigma = s_1 + s_2$. Here J denotes the Bessel function of the first kind. Note that the second line of (33) indicates high-order IMPs. For instance, the 5th IMP at frequency $3\omega_1 + 2\omega_2$ has coefficient $\frac{1}{16} T^2 (3\omega_1 + 2\omega_2)^2 \sigma^2 \mathcal{H}_{32}$.

To provide some insight into the functions $\mathcal{H}_{pq}$ corresponding to low-order intermodulation products, we show in Fig. 7 the functions $\mathcal{H}_{pq}(\lambda)$ up to fifth order, where $\lambda = s_1/\sigma = s_1/(s_1+s_2)$. Note that only the case of odd $p+q$ needs to be considered and that the behavior of the remaining low-order $\mathcal{H}_{pq}$ which are not plotted in Fig. 7 may be inferred from that figure using the relation $\mathcal{H}_{pq}(\lambda) = \mathcal{H}_{qp}(1-\lambda)$. The variable λ represents the relative magnitude of s_1 to the total input signal. Finally, combining (32) and (33) allows us to determine analytically the IMD.

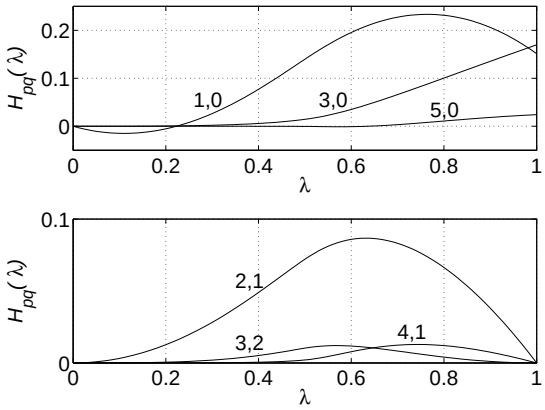

Fig. 7. Plots of the functions $\mathcal{H}_{pq}(\lambda)$ for low-order intermodulation products with odd $p+q$, where $\lambda = s_1/(s_1+s_2)$. Values of p, q are indicated next to each curve.

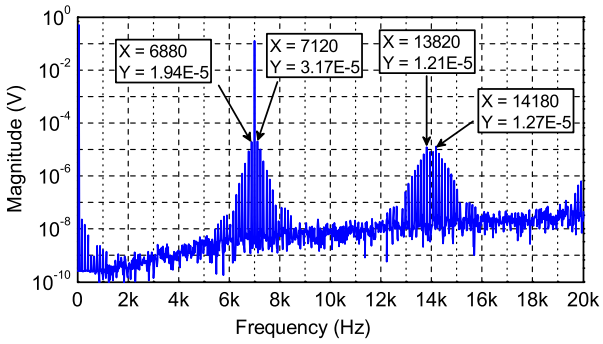

Fig. 8. Frequency spectrum of the output signal for a BD-modulated 2nd-order Class-D amplifier.

The frequency spectrum of the output signal in a typical IMD test is shown in Fig. 8. The two-tone stimulus signals are at 60 Hz and 7 kHz, with the amplitudes equal to 0.5 and 0.125, respectively. Compared to the frequency spectrum of the AD-modulated amplifier shown in [20], there exist significant high-order IMPs in a BD-modulated amplifier, illustrated as the sideband components surrounding the peaks at 7 kHz and 14 kHz. Furthermore, this figure shows that the 5th-order IMPs are even larger than the 3rd-order IMPs at the frequencies surrounding the 2nd-order harmonic of the high-frequency tone (i.e., 14 kHz).

V. Analytical and Simulation Results

In this section, the analysis leading to our expression (23) for the audible output signal of a BD-modulated 2nd-order Class-D amplifier is verified by comparing the derived expressions against computer simulations using both MATLAB Simulink and Cadence Spectre simulators. Since this work focuses on the intrinsic distortion of the BD-modulated Class-D amplifier with the assumption that all the effects of a practical circuit, such as component variation, non-ideality of the output stage and nonlinearity of the low-pass filter,

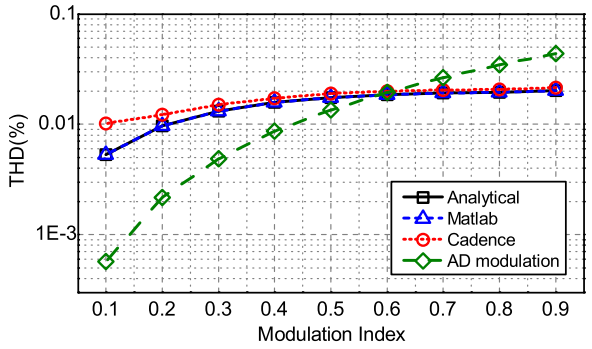

Fig. 9. THD of a BD-modulated 2nd-order Class-D amplifier against the modulation index of the input signal.

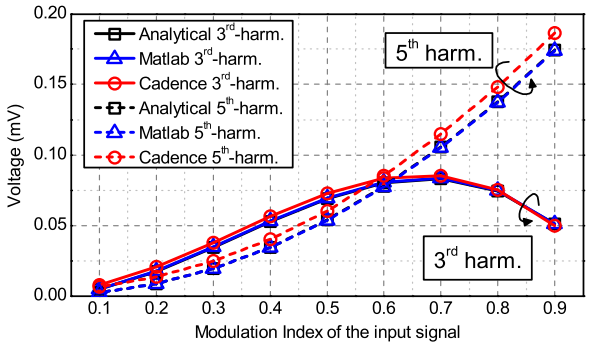

Fig. 10. The 3rd and 5th harmonic components in the demodulated output signal.

are eliminated, no hardware test is required. The Cadence simulation is sufficient to demonstrate the accuracy of the mathematical model derived from the circuit schematic. The second-order loop filter is designed to achieve a high low-frequency gain inside the audio range and the parameter values used are: $c_1 = 498800$ s^{-1}, $c_2 = 490340$ s^{-1}, $T =$ 4e-6 s and $k = 0$. In our Cadence simulations, the power stage is built using a pair of PMOS and NMOS transistors with large W/L ratio, which are simulated using foundry provided BISIM models for the 0.18 μm CMOS process. The fully differential amplifier is created based on a macro model (a single pole system: DC gain = 120 dB and gain-bandwidth product = 100 MHz). The comparator is built using a simple voltage-controlled voltage source. The passive components (capacitors and resistors) are from Cadence analog library. The supply voltage is 3.3 V. As described above, the simulation circuit built in Cadence is quite ideal except for the power MOSFETs.

A. Verification of Total Harmonic Distortion

Fig. 9 presents the THD performance against the modulation index of the input signal. The modulation index ranges from 0.1 to 0.9 and the input signal frequency is set to 3 kHz, so that the high-order harmonic distortions are included. The THD results are calculated based on all the harmonics within the audio range (i.e., from 20 Hz to 20 kHz). The MATLAB simulation results for a 2nd-order Class-D amplifier with binary PWM signal are also provided for comparison. As illustrated in Fig. 9, the matching between the analytical results and the simulation results is excellent; in particular, the MATLAB simulation results and the analytical results are almost indistinguishable. Compared with its AD-modulated counterpart, BD modulation suffers from a much higher THD for small input signal whereas it achieves a better performance for large input signal. Recall that music has a crest factor (i.e., peak to rms ratio) range of 4–10. This means that the modulation index of the input signal in most conditions is around 0.35 or even lower, in which case the AD-modulated Class-D amplifier has a much better performance, compared to BD modulation.

Fig. 10 shows the magnitude of the 3rd- and 5th-harmonic components plotted against the magnitude of the input signal with the same input setting as for Fig. 9. This figure shows that

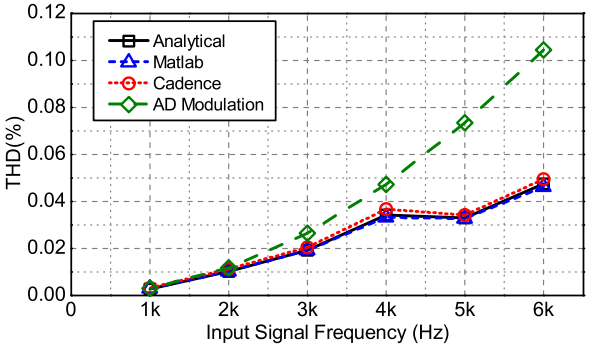

Fig. 11. THD against the frequency of the input signal. The modulation index of the input signal is 0.7.

the analytical results perfectly match the MATLAB simulation results even for individual frequency components and hence demonstrates the accuracy of the analytical expression. The Cadence Spectre simulation results are slightly higher than the analytical predictions and the MATLAB simulation results. This is probably due to the practical limitations of the power MOSFET model employed in the Cadence simulation, such as the on-resistance and the asymmetry of the rising and falling switching edges. As expected from our analysis, the 3rd-order harmonic distortion reaches its peak when the modulation index of the input signal is around 0.7 and then decreases with further increased input signal. On the other hand, the 5th-order harmonic increases quadratically with the magnitude of the input signal and becomes the dominant distortion component for large input signal.

The THD performance against the input signal frequency of the BD-modulated 2nd-order closed-loop Class-D amplifier is given in Fig. 11. The modulation index of the input signal is fixed at 0.7. The input signal frequency is from 1 kHz to 6 kHz. The flattening of the curve between 4 kHz and 5 kHz is due to the fact that the 5th-harmonic distortion for input frequency higher than 4 kHz will fall outside the audio band. As a result, the advantage of lower THD at large modulation index for BD modulation becomes quite obvious for high frequency input signal.

As for the AD-modulated design, the THD of a BD-modulated Class-D amplifier is predicted by the model to be

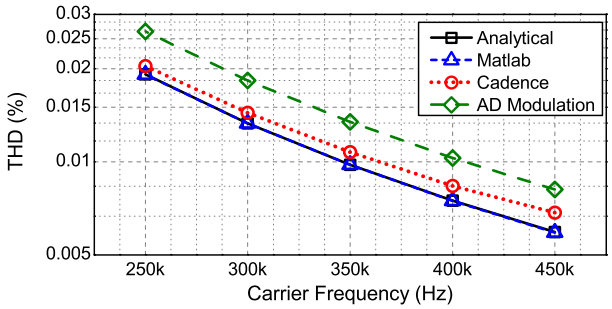

Fig. 12. THD versus carrier frequency. The input signal has $F_{\rm in} = 3$ kHz and $M_{\rm in} = 0.7$.

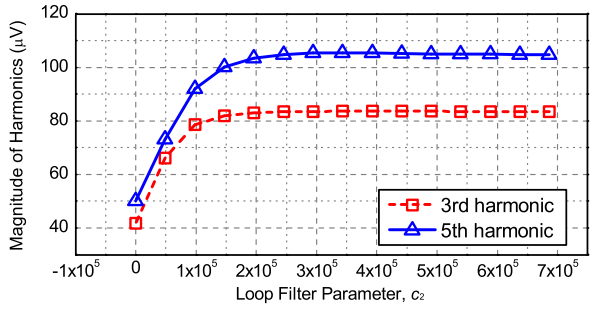

Fig. 13. Harmonic components of a fully differential BD-modulated Class-D amplifier versus the loop filter parameter c_2. The input signal has $F_{\rm in} = 3$ kHz and $M_{\rm in} = 0.7$.

inversely proportional to the square of the switching frequency. This is illustrated in Fig. 12 by the same decreasing slopes for both AD and BD modulations. Note that analytical and MATLAB simulation results are almost indistinguishable. The Cadence simulation results also closely follow the predicted analytical results; the increasing mismatch at higher carrier frequency is probably because of the relative weakening of the intrinsic distortion compared to other sources of distortion.

Fig. 13 illustrates MATLAB simulation results of the significant 3rd and 5th harmonics when the second-order loop filter parameter c_2 reduces from a typical value to 0. It confirms that the harmonic components are independent of the loop filter parameters over a wide range of values, corresponding to normal second-order loop filter design. When c_2 is sufficiently small, however, a dependence on this parameter emerges, and the loop filter becomes close to a first-order design (i.e., the limiting case of $c_2 = 0$ as indicated by the linearized loop gain transfer function, $c_1(s + c_2)/s^2$); in this case, the THD is reduced by half (just as predicted by the output expression of a first-order loop filter design given in (24)).

B. Verification of Intermodulation Distortion

The testing standard set by the Society of Motion Picture and Television Engineers (SMPTE) is applied here to examine the performance of the BD-modulated Class-D amplifier and to verify the accuracy of the analytical output signal expressions. The two-tone input signal consists of a low-frequency high-amplitude tone (60 Hz) and a linearly combined high-frequency tone (7 kHz) at 1/4 the amplitude (12 dB) of

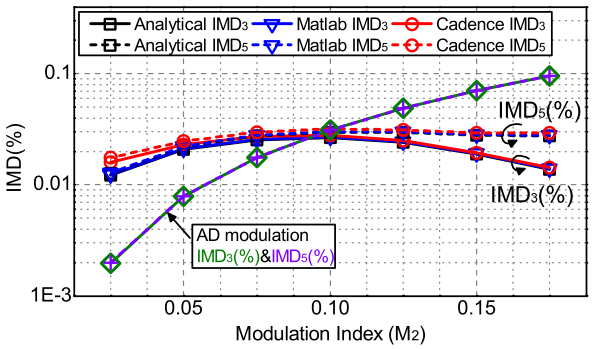

Fig. 14. SMPTE IMD against the modulation index of the high-frequency input signal.

the low-frequency tone [23]; thus $f_1 = \omega_1/2\pi = 60$ Hz, $f_2 = \omega_2/2\pi = 7$ kHz, $s_1 = 4s_2$.

Fig. 14 illustrates the SMPTE IMD of the BD-modulated 2nd-order Class-D amplifier against the modulation index of the high-frequency input component. To ensure that the combined input magnitude is less than 1, the modulation index of the 60 Hz input signal varies from 0.1 to 0.7 and the modulation index of the 7 kHz input signal changes correspondingly from 0.025 to 0.175. Recall that the maximum order of the intermodulation products included for the IMD calculation is indicated by the subscript. For example, IMD_5 means that up to 5th-order IMPs are considered in the calculation. As shown in Fig. 14, the analytical prediction of the IMD is excellent when compared with the MATLAB simulation results. The Cadence simulation results also closely follow the analytical results. The mismatch in the low modulation index range is probably due to the insignificance of the intrinsic intermodulation distortion for small input signal compared to the distortions introduced by other error sources (e.g. the tolerance error of the simulator and the extra distortion caused by the non-ideal power MOSFETs). For instance, due to the low-frequency input signal at 60 Hz, a longer simulation duration is required for frequency analysis, compared to that for THD. Consequently, the error tolerance setting of the Cadence Spectre simulator is relaxed as a trade-off to achieve an affordable simulation time and not to have overloaded simulation data. However, the relaxed tolerance setting limits the accuracy of the Cadence simulation results.

In addition, the MATLAB simulated IMD_3 and IMD_5 results for AD modulation are also shown in Fig. 14. As is the case for THD, BD modulation achieves smaller IMD for large input signal, but has larger IMD for small input signal, compared to AD modulation. The crossing point for equal IMD performance is around $M_2 = 0.1$ (i.e., the summed magnitude for the two-tone signals is equal to 0.5, half the full input signal swing). It may also be worthwhile to highlight that, for AD modulation, the IMD_5 almost overlaps with the IMD_3, which shows that 5th-order IMPs at the output of an AD-modulated Class-D amplifier are insignificant and can be ignored when compared to 3rd-order IMPs.

Fig. 15 plots the magnitude of the typical 3rd and 5th-order IMPs for BD modulation against the modulation index

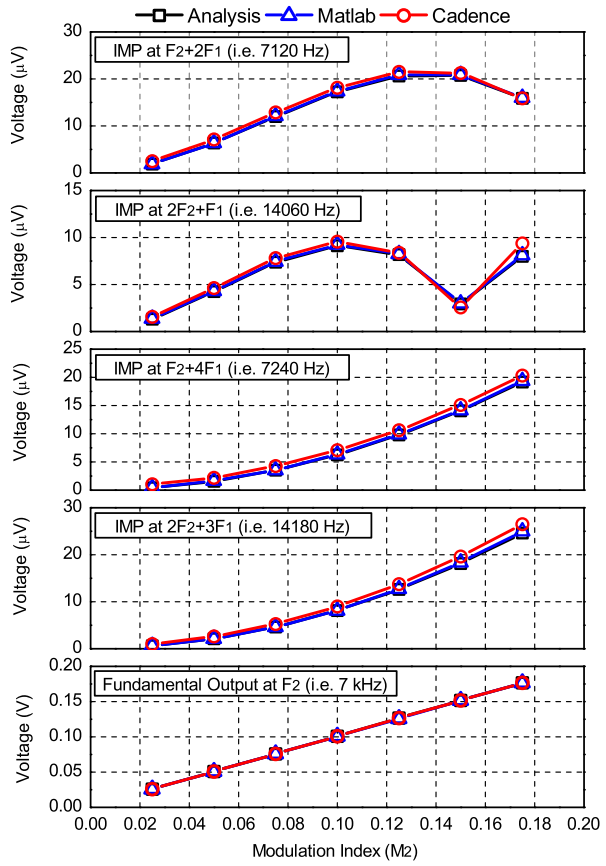

Fig. 15. The IMPs along with the high frequency fundamental output compoment against the modulation index of the high frequency input signal.

of the high-frequency input signal, M_2, with the same input setting as Fig. 14. Note that only the IMPs at frequency equal to $nf_2 + mf_1$ are shown here, as the remaining IMPs at frequency $nf_2 - mf_1$ have similar patterns to their respective counterparts. It is clear that the analytical expression accurately predicts the dependency of each individual frequency component for a range of values of M_2. Note that the 3rd-order IMP at frequency $f_2 + 2f_1$ has a roughly parabolic response against the magnitude of the input signal, whereas the 3rd-order IMP at frequency $2f_2 + f_1$ has a fluctuating response, i.e., rising to a peak when M_2 increases to 0.1, followed by a trough at $M_2 \approx 0.15$. As a result, IMD_3 in Fig. 14 is noted to decrease when M_2 is higher than a certain value, approximately 0.1. On the other hand, the 5th-order IMPs increase monotonically with respect to M_2 and dominate the intrinsic distortion of the amplifier for large input signal. This is reflected in Fig. 14 as the IMD_5 is significant larger than the IMD_3 for M_2 beyond 0.1.

VI. Conclusions

In this paper, we have presented a comprehensive mathematical analysis of the intrinsic distortion of a BD-modulated closed-loop Class-D amplifier. The derived analytical expression accurately predicts the audio components of the frequency spectrum of the output signal and is applicable to any band-limited input signal. For the special case of either single-tone or two-tone input signals, the analytical expression clearly demonstrates the unique intrinsic distortion properties of a BD-modulated design, as compared to its AD-modulated counterpart. More precisely, it shows that the 3rd-order harmonic and intermodulation products for BD modulation have a roughly parabolic response as a function of the magnitude of the input signal. Furthermore, there exist significant high-order distortion components in the output spectrum for BD modulation, in the form of the 5th-order harmonic and 5th-order intermodulation products, compared to AD modulation. This may be a potential drawback of BD modulation as human beings are quite sensitive to such high-order distortion.

Appendix

To derive the intermodulation products generated by the term $\frac{1}{16}T^2(s^2(t))''\operatorname{sgn}(s(t))$ in the second line of (23), we begin by introducing a constant σ, which is arbitrary, except that $\sigma \geq s_1 + s_2$. Then we define a function $H(s)$, given by

$$H(s) = s^2 \operatorname{sgn}(s) \qquad \text{for } |s| < \sigma, \tag{35}$$

together with the periodicity condition $H(s + 2\sigma) = H(s)$. This function may be represented by the Fourier series

$$H(s) = \sigma s + \sum_{\substack{n=-\infty \\ n\,\text{odd}}}^{\infty} \frac{4\mathrm{j}\sigma^2}{n^3\pi^3} \mathrm{e}^{n\mathrm{j}\pi s/\sigma}. \tag{36}$$

Now we see that, for a two-tone input signal signal of the form $s(t) = s_1 \sin\omega_1 t + s_2 \sin\omega_2 t$, $H(s)$ can be expressed as

$$H(s(t)) = \sigma s(t) + \sum_{p=-\infty}^{\infty} \sum_{q=-\infty}^{\infty} H_{pq} \mathrm{e}^{\mathrm{j}\Omega_{pq} t}, \tag{37}$$

where

$$H_{pq} = \sum_{\substack{n=1 \\ n\,\text{odd}}}^{\infty} \frac{8\mathrm{j}\sigma^2}{n^3\pi^3} \mathrm{J}_p(n\pi s_1/\sigma)\mathrm{J}_q(n\pi s_2/\sigma), \tag{38}$$

$\Omega_{pq} = p\omega_1 + q\omega_2$ and J denotes the Bessel function of the first kind. In deriving (37), we use the Jacobi–Anger result [24]

$$\mathrm{e}^{\mathrm{j}z\sin\theta} = \sum_{m=-\infty}^{\infty} \mathrm{J}_m(z)\mathrm{e}^{m\mathrm{j}\theta}. \tag{39}$$

Note that, despite superficial appearances, once the infinite sums are taken in (37), *the final answer is independent of the choice of* σ: thus equation (37) holds for *any* $\sigma \geq s_1 + s_2$. To simplify our presentation, we have set $\sigma = s_1 + s_2$ in Section IV.

References

[1] M. Berkhout and L. Dooper, *Class-D audio amplifiers in mobile applications*, IEEE Trans. Circuits Systems I, vol. 57, pp. 992–1002, 2010.

[2] J. D. Martin, *Theoretical efficiencies of class D power amplifiers*, Proc. IEE, vol. 117, no. 6, pp. 1089-1090, Jun. 1970.

[3] M. A. Teplechuk, A. Gribben and C. Amadi, *True filterless class-D audio amplifier*, IEEE J. Solid-State Circuits, vol. 46, pp. 2784-2793, 2011.

[4] Y. Choi, W. Tak, Y. Yoon, J. Roh, S. Kwon, and J. Koh, *A 0.018% THD+N, 88-dB PSRR PWM class-D amplifier for direct battery hookup*, IEEE J. Solid-State Circuits, vol. 47, pp. 454-463, 2012.

[5] W. H. GROENEWEG, *Analog signal processing for a class D audio amplifier in* 65 *nm CMOS technology*, in Proc. ESSCIRC, 2008, pp. 322-325.
[6] R. BEAN, R. LIND, AND R. KEHR, *An integrated* 40 *W analog input class D amplifier with improved clipping recovery and reduced turn-on transients*, in AES 27th international Conference, Copenhagen, Denmark, 2005.
[7] L. RISBO AND C. NEESGAARD, *PWM amplifier control loops with minimum aliasing distortion*, in AES 120th Convention, Paris, France, 2006.
[8] B. H. CANDY AND S. M. COX, *Improved analogue class-D amplifier with carrier symmetry modulation*, in AES 117th Convention, San Francisco, CA, USA, 2004.
[9] J. YU, M. T. TAN, S. M. COX AND W. L. GOH, *A dual-feedforward carrier-modulated second-order class-D amplifier with improved THD*, IEEE Trans. Circuits and Systems II: Exp. Briefs, vol. 59, pp. 35-39, 2012.
[10] S. M. COX AND B. H. CANDY, *Class-D audio amplifiers with negative feedback*, SIAM J. Appl. Math., vol. 66, pp. 468–488, 2005.
[11] H. S. BLACK, *Modulation Theory*, New York: Van Nostrand Reinhold Company, 1953, pp. 263–281.
[12] Z. SONG AND D. V. SARWATE, *The frequency spectrum of pulse width modulated signals*, Signal Processing, vol. 83, pp. 2227–2258, 2003.
[13] M. T. TAN, J. S. CHANG, H. C. CHUA, AND B. H. GWEE, *An investigation into the parameters affecting total harmonic distortion in low-voltage low-power class-D amplifiers*, IEEE Trans. Circuits Systems I, vol. 50, pp. 1304–1315, 2003.
[14] S. M. COX, M. T. TAN AND J. YU, *A second-order class-D audio amplifier*, SIAM J. Appl. Math., vol. 71, pp. 270–287, 2011.
[15] W. SHU AND J. S. CHANG, *THD of closed-loop analog PWM class-D amplifiers*, IEEE Trans. Circuits and Systems I: Reg. Papers, vol. 55, pp. 1769-1777, 2008.
[16] B. PUTZEYS, *Globally modulated self-oscillating amplifier with improved linearity*, in AES 37th International Conference, Hillerød, Denmark, 2009.
[17] S. K. MAZUMDER, A. H. NAYFEH AND D. BOROYEVICH, *Theoretical and experimental investigation of the fast- and slow-scale instabilities of a DC–DC converter*, IEEE Trans. Power Electronics, vol. 16, pp. 201–216, 2001.
[18] S. K. MAZUMDER, A. H. NAYFEH AND D. BOROYEVICH, *An investigation into the fast- and slow-scale instabilities of single phase bidirectional boost converter*, IEEE Trans. Power Electronics, vol. 18, pp. 1063–1069, 2003.
[19] C. PASCUAL, Z. SONG, P. T. KREIN, D. V. SARWATE, P. MIDYA, AND W. J. ROECKNER, *High-fidelity PWM inverter for digital audio amplification: spectral analysis, real-time DSP implementation, and results*, IEEE Trans. Power Electronics, vol. 18, pp. 473–485, 2003.
[20] J. YU, M. T. TAN, S. M. COX AND W. L. GOH, *Time-domain analysis of intermodulation distortion of closed-loop Class D amplifiers*, IEEE Trans. Power Electron., vol. 27, pp. 2453-2461, 2012.
[21] W. R. BENNETT, *New results in the calculation of modulation products*, Bell Syst. Tech. J., vol. 12, pp. 228–243, 1933.
[22] W. R. BENNETT, *The biased ideal rectifier*, Bell Syst. Tech. J., vol. 26, pp. 139–169, 1947.
[23] B. METZLER, Audio Measurement Handbook, Audio Precision Inc., 1993.
[24] G. N. WATSON, *A treatise on the theory of Bessel functions*, Cambridge University Press, Cambridge, 2nd ed., 1944.